

OBSERVATIONAL CONSTRAINTS ON THE PULSAR WIND MODEL: THE CASES OF CRAB AND VELA

JAZIEL G. COELHO^{1,2}, JOSÉ C. N. DE ARAUJO², SAMANTHA M. LADISLAU² AND RAFAEL C. NUNES²

Draft version March 19, 2022

ABSTRACT

As is well known, pulsars are extremely stable rotators. However, although slowly, they spin down thanks to brake mechanisms, which are in fact still subject of intense investigation in the literature. Since pulsars are usually modelled as highly magnetized neutron stars that emit beams of electromagnetic radiation out of their magnetic poles, it is reasonable to consider that the spindown has to do with a magnetic brake. Although an interesting and simple idea, a pure magnetic brake is not able to adequately account for the spindown rate. Thus, many alternative spindown mechanisms appear in the literature, among them the pulsar wind model, where a wind of particles coming from the pulsar itself can carry part of its rotational kinetic energy. Such a spindown mechanism depends critically on three parameters, namely, the dipole magnetic field B , the angle between the magnetic and rotation axes (ϕ), and the density of primary particles (ζ) of the pulsar's magnetosphere. Differently from a series of articles in this subject, we consider for the first time in the literature a statistical modelling which includes a combination of a dipole magnetic and wind brakes. As a result, we are able to constrain the above referred parameters in particular for Crab and Vela pulsars.

Subject headings: pulsars: individual (PSR B0833-45, PSR B0531+21) – stars: fundamental parameters – stars: neutron

1. INTRODUCTION

As is well known, Pulsars, which is usually associated with rotating neutron stars (NSs), have extremely stable rotating periods. In particular the so-called rotation-powered pulsars (RPPs) emit radiation by means of their rotational kinetic energies, as a result their periods increase, i.e., they spindown (Ostriker & Gunn 1969; Gunn & Ostriker 1969). The electromagnetic energy emitted by a pulsar, in this case, come from its rotational kinetic energy (see e.g., Landau & Lifshitz 1975; Padmanabhan 2001).

It is very likely that pulsars, due to their dynamic nature, should always present important temporal changes in some astrophysical quantities. In particular, increases in the rotational periods, for example, are usually quite small. The Crab Pulsar (PSR B0531+21), for example, which has a period of ~ 33 ms, has a period increase rate of $\approx 4.2 \times 10^{-13}$ s/s. While the Vela Pulsar (PSR J0835-4510 or PSR B0833-45) has a spin period of ~ 89 ms and a spindown rate of $\approx 1.25 \times 10^{-13}$ s/s⁴.

A long standing issue is to understand how exactly the pulsars spindown. The magnetic dipole radiation model is a simple and interesting proposal to explain the spindown. However, such a model predict that the brake index, a dimensionless quantity that relates the period and its first and second time derivatives, is exactly equal to three, which is not observationally corroborated. In addition to that, the estimation of the dipole magnetic field is subject to several uncertainties. For instance, several analysis suggests that should not be disregard the possibility of multipolar magnetic field in highly magnetized stars (see, e.g., de Lima et al. 2020). Indeed, NICER's

X-ray data from PSR J0030+0451 has recently led to the first map of the hot spots on the surface of a star (see Riley et al. 2019; Bogdanov et al. 2019). The hot spots are far from antipodal, meaning that the magnetic field structure of a pulsar is much more complex.

The fact that no pulsar has a braking index equal to three implies the need to consider more elaborate spindown models. One such a model is the so-called pulsar wind model (see Xu & Qiao 2001; Kou & Tong 2015; Tong & Kou 2017), which we consider in the present work. We shall see later in this paper that different values of braking index is naturally the case whenever pulsar wind mechanism also features in the energy loss budget of pulsars, along with the classic magnetic dipole radiation. In addition, observations of intermittent pulsars showed explicitly the substantial role of particle wind in pulsar spindown (see Kramer et al. 2006). Magnetohydrodynamics simulations also found similar expressions to the wind braking model (see e.g., Spitkovsky 2006). In the next section, we briefly review such a model.

It is worth mentioning that there are several scenarios that challenge the classic magnetic dipole model, like the one involving the accretion of fall-back material via a circumstellar disk (Chen & Li 2016), and modified canonical models to explain the observed braking index ranges (see Allen & Horevath 1997; Magalhaes et al. 2012; Ekji et al. 2016; de Araujo et al. 2016a,b,c, 2017, among others, and references therein for further models). Another interesting model for the brake is the quantum vacuum friction. We refer the reader to Coelho et al. (2016) for details. Therefore, energy loss mechanisms for pulsars are still under continuous debate.

As already mentioned we consider here the pulsar wind model, but following a different approach than that usually adopted in the literature. By means of a statistical model, we analyze in particular three relevant parameters of the wind model, namely, B , ϕ , ζ , the dipole magnetic field, the initial angle between the rotation and magnetic axes, and the parameter related to the density of primary particles of the magnetosphere, respectively.

The present paper is organized as follows. In Section 2,

¹ Departamento de Física, Universidade Tecnológica Federal do Paraná, 85884-000 Medianeira, PR, Brazil

² Divisão de Astrofísica, Instituto Nacional de Pesquisas Espaciais, Avenida dos Astronautas 1758, 12227-010, São José dos Campos, SP, Brazil
jazielfcoelho@utfpr.edu.br

⁴ For information about pulsars, we refer the reader to the ATNF catalog available at: <https://www.atnf.csiro.au/research/pulsar/psrcat/>

we revise the pulsar wind model, in Section 3, we present the statistical model to analyze the parameters B , ϕ and ζ for the Crab and Vela pulsars. The results and discussions are presented in Section 4. The main conclusions are summarized in Section 5.

2. PULSAR WIND MODEL

In this section we briefly review the pulsar wind model as originally put forward by Xu & Qiao (2001) in order to elucidate the physical ideas involved.

Let us consider the pulsar as an oblique rotator that has two components of magnetic dipole: one parallel and other perpendicular to the axis of rotation of the pulsar. The perpendicular component is responsible for the energy loss by the magnetic dipole radiation (see e.g., Landau & Lifshitz 1975; Padmanabhan 2001), whereas the parallel component is related to the acceleration of particles (see Li et al. 2014). Then, the phenomenon of pulsar wind is basically an energy loss mechanism due to the classic magnetic dipole radiation and particle acceleration (see Kou & Tong 2015; Tong & Kou 2017).

The energy loss due to particle wind depends on the so-called acceleration potential drop, Δv , given by (Xu & Qiao 2001)

$$\dot{E}_{\text{wind}} = 2\pi r_p^2 \rho_e \Delta v, \quad (1)$$

where $r_p = R(R\Omega/c)^{1/2}$ is polar gap radius, c is the speed of light, ρ_e is the primary particle density, and Δv is the corresponding acceleration potential in the acceleration gap. The density of primary particles is related to the Goldreich–Julian charge density by $\rho_e = \zeta \rho_{GJ}$ (Goldreich & Julian 1969), being ζ a coefficient which can be constrained by observations. It is important to note that ζ is related to the primary particles in the acceleration gap but not to the total outflow particles.

Notice that the presence of the acceleration potential can accelerate primary particles. Secondary particles are generated subsequently. Meanwhile, the density of secondary particles can be much higher than the Goldreich–Julian density. In the wind braking model, all the particles injected into the magnetosphere from the acceleration region are defined as primary particles.

If we assume that the maximum potential for a rotating dipole is given by $\Delta v = \mu\Omega^2/c^2$, it can be shown that the rotational energy loss rate reads

$$\dot{E}_{\text{wind}} = \frac{2\mu^2\Omega^4}{3c^3} 3\zeta \frac{\Delta v}{\Delta v} \cos^2 \phi, \quad (2)$$

where $\mu = 1/2BR^3$ is the magnetic dipole moment (B is the magnetic field strength at the magnetic pole of the star and R is the neutron star radius), Ω is the rotational frequency, and ϕ the inclination angle between rotation and magnetic axes.

On the other hand, as it is well known, pulsars also lose energy via the classic magnetic dipole radiation (Padmanabhan 2001; Landau & Lifshitz 1975). The magnetic dipole radiation and the outflow of particle wind may contribute independently. Then, the total rotational energy loss rate is given by (Kou & Tong 2015; Tong & Kou 2017)

$$\dot{E} = \frac{2\mu^2\Omega^4}{3c^3} \left(\sin^2 \phi + 3\zeta \frac{\Delta v}{\Delta v} \cos^2 \phi \right) = \frac{2\mu^2\Omega^4}{3c^3} \chi. \quad (3)$$

We note that if the acceleration potential $\Delta v = 0$, there are no particles accelerated in the gap, the pulsar is just braking down by the magnetic dipole radiation. Here χ is a dimensionless function that can be viewed as the dimensionless spin-down

torque. The expressions of χ for different acceleration models had been very well studied by Kou & Tong (2015) [see Table 2 therein for various acceleration models]. In fact, the χ parameter depends on the particle acceleration model adopted. Here, we will use the vacuum gap (VG) model with curvature radiation (CR) (see Ruderman & Sutherland 1975).

We shall surmise in this work that the total energy of the star is provided by its rotational counterpart, $E_{\text{rot}} = I\Omega^2/2$, and its change is attributed to both \dot{E}_{wind} and the magnetic dipole radiation. Thus, from Eq 3, the evolution of the rotational frequency of a star is given by

$$\dot{\Omega} = -\frac{B^2 R^6 \Omega^3}{6Ic^3} \chi_{\text{VG}}^{\text{CR}}, \quad (4)$$

with

$$\chi_{\text{VG}}^{\text{CR}} = \sin^2 \phi + \begin{cases} 4.96 \times 10^2 \zeta \left(1 - \frac{\Omega_{\text{death}}}{\Omega}\right) B_{12}^{-8/7} \Omega^{-15/7} & \text{if } \Omega > \Omega_{\text{death}} \\ 0 & \text{if } \Omega < \Omega_{\text{death}}, \end{cases} \quad (5)$$

where the term in parentheses account for the pulsar death, and B_{12} is the surface magnetic field in units of 10^{12} G. Notice that in the above equation, the term $\cos^2 \phi$, which appears in Eq 2, is now omitted. In Tong & Kou (2017), the authors argue that $\cos^2 \phi$ may not appear, in accordance with magnetospheric simulations performed by Li et al. (2012).

Consequently, the effect of pulsar death can be incorporated in the rotational energy loss rate and must be considered in modelling the long-term rotational evolution of the pulsar. Note that when a pulsar is dead ($\Omega < \Omega_{\text{death}}$), it is braked only by magnetic dipole radiation, i.e., $\chi_{\text{VG}}^{\text{CR}} = \sin^2 \phi$. Then, following the same procedure of (Contopoulos & Spitkovsky 2006; Kou & Tong 2015), the death period ($P_{\text{death}} = 2\pi/\Omega_{\text{death}}$) is defined as

$$P_{\text{death}} = 2.8 \left(\frac{B}{10^{12} \text{G}} \right)^{1/2} \left(\frac{V_{\text{gap}}}{10^{12} \text{V}} \right)^{-1/2} \text{ s}. \quad (6)$$

The inclination angle ϕ is allowed to evolve over time, and following Tong & Kou (2017), the evolution of ϕ reads

$$\dot{\phi} = -\frac{B^2 R^6 \Omega^2}{6Ic^3} \sin \phi \cos \phi \quad (7)$$

As already mentioned, the energy carried away by the dipole radiation and the relativistic particles originates from the rotational kinetic energy, the loss rate of which is $I\Omega\dot{\Omega}$.

Recall that the braking index is defined by,

$$n = \frac{\Omega \ddot{\Omega}}{\dot{\Omega}^2}. \quad (8)$$

It is interesting to note that the braking index implicitly depends on the magnetic field B , the inclination angle ϕ , and particle density ζ .

3. STATISTICAL MODEL FOR CRAB AND VELA

In Kou & Tong (2015) and, in particular and mainly in Tong & Kou (2017), one sees that the key parameters to appropriately model the pulsar spindown when considering a combination of magnetic dipole and particle wind brakes are B , ϕ and ζ .

In a modelling for the Crab pulsar, Kou & Tong (2015) assume that $B = 8.1 \times 10^{12}$ G, $\phi = 55^\circ$ and $\zeta = 10^3$. Later, Tong & Kou (2017) adopt $B \sim 10^{12}$ G, $\phi = 60^\circ$ and $\zeta = 10^2$. The

authors argue that the primary particle density, ρ_e , of young pulsars is at least 80 times the ρ_{GJ} in the vacuum gap model. In fact, the particle density in the accelerating region could be $\sim 10^3$ to 10^4 times the Goldreich–Julian charge density (see also Yue et al. 2007). A much larger particle density than the Goldreich–Julian density in the pulsar magnetosphere is also found in other models and observations (Kou & Tong 2015; Tong & Kou 2017, and references therein).

Differently from these and other previous studies, we consider for the first time in the literature a statistical modelling which includes a combination of a dipole magnetic and wind brakes. We argue that a robust way to adequately obtain and constrain ϕ , ζ and B is by mean of statistical analysis.

According to the inferred observational range of inclination angles and characteristic magnetic fields, we are able to constrain the range of values of ϕ and ζ for a particular pulsar. As a first application of our modelling we consider the widely known Crab and Vela pulsars.

Here, we use the Markov Chain Monte Carlo (MCMC) method to analyze the parameters $\theta_i = \phi, \zeta, B$, building the posterior probability distribution function

$$p(D|\theta) \propto \exp\left(-\frac{1}{2}\chi^2\right), \quad (9)$$

where

$$\chi^2 = \left(\frac{n - n_{th}}{\sigma_n}\right)^2, \quad (10)$$

where n , n_{th} and σ_n are the observed braking index (median value), theoretical braking index and the uncertainties of the observed braking index (see Table 1), respectively.

The goal of any MCMC approach is to draw M samples θ_i from the general posterior probability density

$$p(\theta_i, \alpha|D) = \frac{1}{Z} p(\theta, \alpha) p(D|\theta, \alpha), \quad (11)$$

where $p(\theta, \alpha)$ and $p(D|\theta, \alpha)$ are the prior distribution and the likelihood function, respectively. Here, the quantities D and α are the set of observations and possible nuisance parameters. The amount Z is a normalization term. In order to constrain the baseline θ_i , let us assume estimates of the braking index parameters for the pulsars as follows: $n = 2.51 \pm 0.01$ for Crab and $n = 1.4 \pm 0.2$ for Vela (see Table 1).

We perform the statistical analysis based on the *emcee* algorithm (see Foreman-Mackey et al. 2013), assuming the theoretical model described in Sec. 2 and the following priors on the parameters baseline: first, we analyze both Vela and Crab with a uniform prior on the inclination angle to be $\phi \in [45^\circ, 70^\circ]$, which are consistent with observational constraints (Lyne et al. 2013). As a second case, we consider a uniform prior $\phi \in [70^\circ, 90^\circ]$. In fact, the shape of the beam of the Crab pulsar has been investigated over the past few years, resulting in a range of estimates of $\phi \in [45^\circ, 70^\circ]$ (see e.g., Dyks & Rudak 2003; Harding et al. 2008; Watters et al. 2009; Du et al. 2012). Unfortunately, at present it is impossible to accurately determine the inclination angle of individual pulsars. Therefore, these issues are still under continuous debate (see e.g., Lander & Jones 2018; Novoselov et al. 2020).

From the profile modeling, we can already get some information about the inclination angle. In fact, the braking index is not the only observational input, since preliminary information on ϕ is already known. Thus, we use this information as uniform prior in our analysis. We are fitting the theoretical model

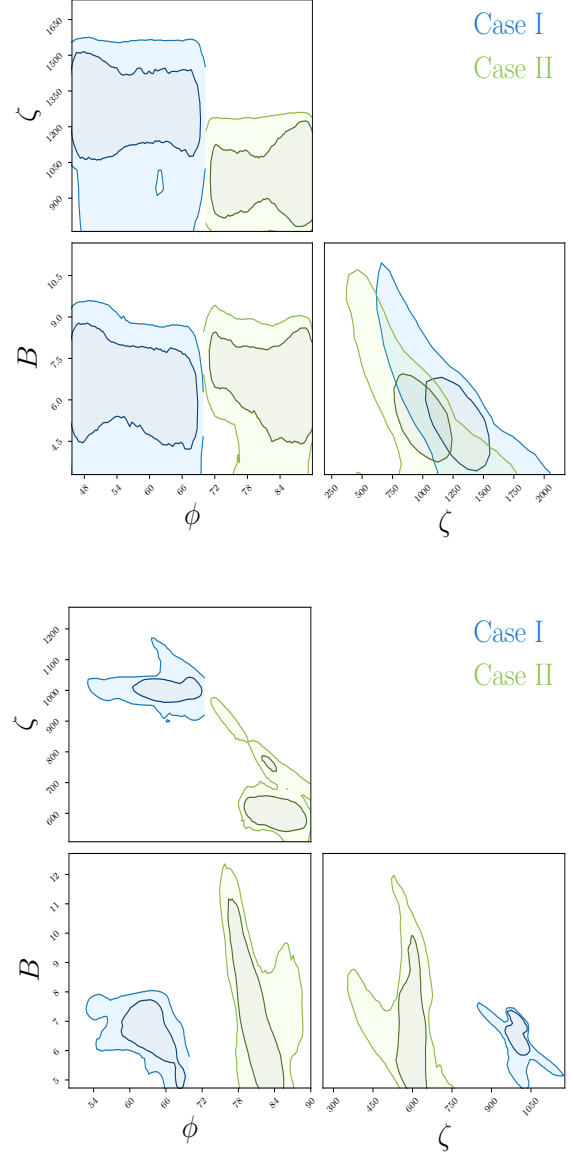


FIG. 1.— The parametric space at 38% CL and 68% CL, under the prior consideration $\phi \in [45^\circ, 70^\circ]$ (Case I) and $\phi \in [70^\circ, 90^\circ]$ (Case II). Upper panel: Vela Pulsar. Lower panel: Crab Pulsar. The parameter B is in units of 10^{12} G.

under an observational information quantified in terms of n , which represents in practical terms just one data point, with already known information on ϕ . Thus, we will maintain a conservative statistical limit in our results, and we will quantify our all analysis at 38% ($\sim 0.5\sigma$) and 68% ($\sim 1\sigma$) CL. In what follows, let us present a summary of our main results.

4. RESULTS AND DISCUSSIONS

In the following we explore the parameter space ϕ , ζ and B with our MCMC approach, in order to constrain the probability distribution of these parameters that characterize the pulsar wind model. Then, we relaxed the value of B using a uniform prior with $B \in [1, 100]$ in units of 10^{12} G. As a case study, in Fig. 1 we show the parametric space on the plan ϕ – ζ at 38% and 68% confidence level (CL), assuming $\phi \in [45^\circ, 70^\circ]$ (Case I) and $\phi \in [70^\circ, 90^\circ]$ (Case II).

The age of a pulsar is a useful parameter, but it is difficult

TABLE 1
PERIOD (P), ITS FIRST DERIVATIVE (\dot{P}), SURFACE MAGNETIC FIELD (B), BRAKING INDEX (n) AND SPINDOWN (SD) AGE FOR THE VELA AND CRAB PULSARS.

| Pulsar | P (s) | \dot{P} (10^{-13} s/s) | B (10^{12} G)* | n | age (kyr)** | Ref. |
|---------------------|---------|-----------------------------|---------------------|-----------------|-------------|--|
| PSR B0833-45 (Vela) | 0.089 | 1.25 | 6.8 | 1.4 ± 0.2 | 11.3 | Lyne et al. (1996); Espinoza et al. (2017) |
| PSR B0531+21 (Crab) | 0.033 | 4.21 | 7.5 | 2.51 ± 0.01 | 0.967 | Lyne et al. (1993, 2015) |

* $B = 6.4 \times 10^{19} \sqrt{P\dot{P}}$ G - for canonical parameters of M , R and I .

** For the Vela pulsar we use the spindown age = $P/2\dot{P}$. However, we have adopted the true age for Crab pulsar, which is known to be just 967 yr because the Crab supernova was observed in 1054 AD.

to get the age from observations. Here, we have used the values showed in Table 1. For the Vela pulsar we adopted the spindown age. This age is in good agreement with independent age estimators (e.g., proper motion and SNR age). It is worth mentioning that the different age estimates for both pulsars do not practically influence our statistical modeling.

For the Vela pulsar, we find $\zeta = 1280^{+350}_{-630}$ and $\zeta = 990^{+320}_{-570}$ at 1σ CL from the Case I and II, respectively. For this inference, we find $B = 6.5^{+3.1}_{-4.4} \times 10^{12}$ G and $B = 6.8^{+2.5}_{-5.1} \times 10^{12}$ G for the the Case I and II, respectively. Now, for the Crab pulsar, we find $\zeta = 1002^{+83}_{-76}$ and $\zeta = 600^{+160}_{-100}$ at 1σ CL from the Case I and II, respectively, with $B = 6.6^{+1.2}_{-1.7} \times 10^{12}$ G and $B = 7.3^{+2.1}_{-4.3} \times 10^{12}$ G from the case I and II, respectively. Note that the mean value of the B parameter can present statistical fluctuations along the MCMC analysis. But, as expected, these fluctuations are completely compatible with the input value. As previous mentioned the characteristic (inferred) magnetic field from the classical magnetic dipole radiation is subject to some uncertainties. To take into account the magnetic field effects in our results, we have relaxed B using a uniform prior with $B \in [1, 100]$ in units of 10^{12} G. Nevertheless, it is worth mentioning that up to now, attempts to estimate the magnetic field strength in isolated pulsars through the measurement of cyclotron resonance features, as successfully done for accreting pulsars, have been inconclusive.

Fig. 2 shows the reconstruction at 1σ CL of the braking index n as a function of time for Vela and Crab, on the left and right panel, respectively. The reconstruction is done applying standard propagation of error on Eq. (8) from the best fit values obtained in our analysis within the case $\phi \in [45^\circ, 70^\circ]$. Fig. 3 shows the reconstruction for the second case, $\phi \in [70^\circ, 90^\circ]$. In all of our analysis, we discard the first 10% steps of the chain as burn-in. We follow the Gelman-Rubin convergence criterion (Gelman & Rubin 1992), checking that all parameters in our chains had good convergence.

5. FINAL REMARKS

There are in the literature several alternatives to the magnetic dipolar brake to explain the pulsar spindown, among them the pulsar wind model, where a wind of particles coming from the pulsar itself can carry part of its rotational kinetic energy. We have seen that such a spindown mechanism depend critically on three parameters, namely, the dipole magnetic field, the angle between the magnetic and rotation axes, and the density of primary particles of the pulsar's magnetosphere.

Differently from a series of previous articles in this subject, we consider for the first time in the literature a statistical modelling which includes a combination of a dipole magnetic and particle wind brakes. Although in general there is a dependence of all the parameters on the pulsars, we used here, without loss of generality and for the sake of exemplification, only the vacuum gap model for the particle acceleration. We emphasize that this same approach can be applied regardless of the choice of the acceleration model. As a result, we are

able to constrain the three relevant parameters of this model, i.e., B , ϕ and ζ , in particular for Crab and Vela pulsars. This study ought to lay the groundwork for future research on the fundamental parameters of pulsar wind model and also particle acceleration.

ACKNOWLEDGEMENTS

The authors thank the referee for comments which helped to improve the quality of the manuscript. J.G.C. is likewise grateful to the support of CNPq (421265/2018-3 and 305369/2018-0) and FAPESP Project No. 2015/15897-1. J.C.N.A. thanks FAPESP (2013/26258-4) and CNPq (308367/2019-7) for partial financial support. R.C.N. would like to thank the agency FAPESP for financial support under the project No. 2018/18036-5.

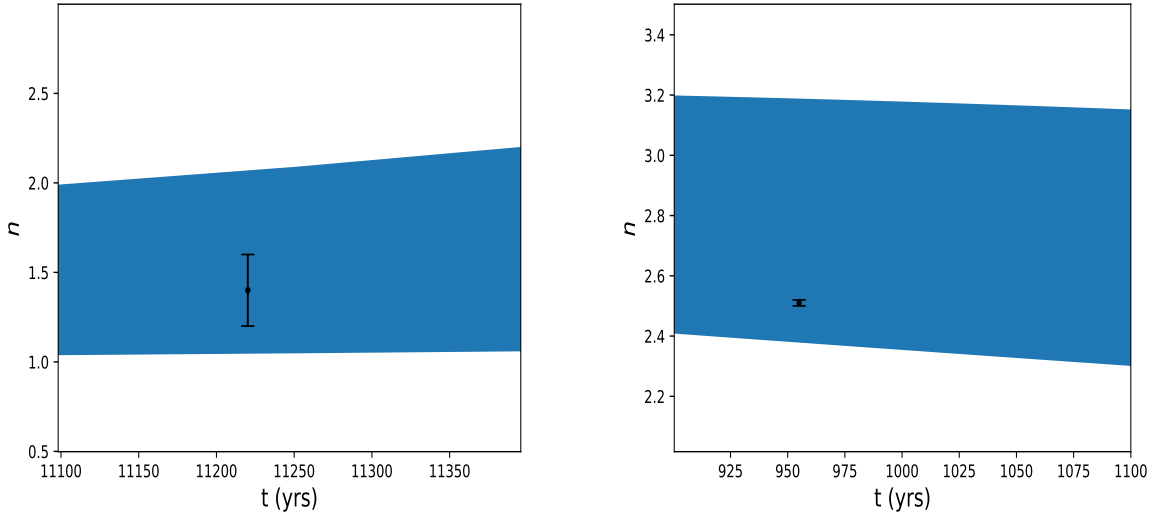


FIG. 2.— Statistical reconstruction at 1σ CL of the braking index n as a function of time for Vela and Crab, on the left and right panel, respectively (Case I). The error bar in black represent the n measurements.

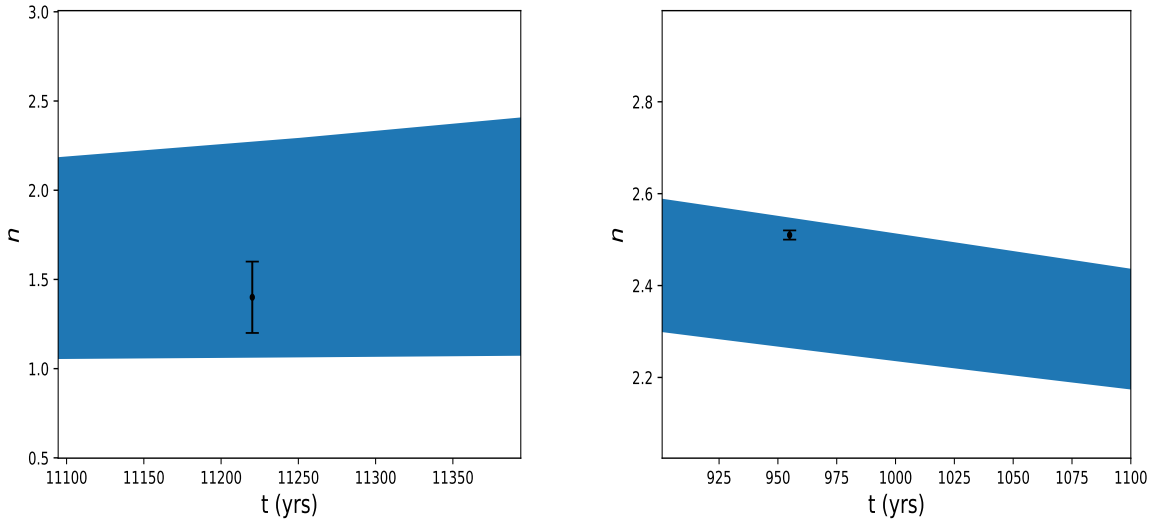


FIG. 3.— Statistical reconstruction at 1σ CL of the braking index n as a function of time for Vela and Crab, on the left and right panel, respectively (Case II). The error bar in black represent the n measurements.

REFERENCES

- Allen, M. P., & Horvath, J. E. 1997, *ApJ*, 488, 409
- Bogdanov, S., Lamb, F. K., Mahmoodifar, S., et al. 2019, *ApJL*, 887, L26
- Chen, W.-C., & Li, X.-D. 2016, *MNRAS*, 455, L87
- Coelho, J. G., Pereira, J. P., & de Araujo, J. C. N. 2016, *ApJ*, 823, 97
- Contopoulos, I., & Spitkovsky, A. 2006, *ApJ*, 643, 1139
- de Araujo, J. C. N., Coelho, J. G., & Costa, C. A. 2016a, *JCAP*, 2016, 023
- . 2016b, *ApJ*, 831, 35
- . 2016c, *European Physical Journal C*, 76, 481
- . 2017, *European Physical Journal C*, 77, 350
- de Lima, R. C. R., Coelho, J. G., Pereira, J. P., Rodrigues, C. V., & Rueda, J. A. 2020, *ApJ*, 889, 165
- Du, Y. J., Qiao, G. J., & Wang, W. 2012, *ApJ*, 748, 84
- Dyks, J., & Rudak, B. 2003, *ApJ*, 598, 1201
- Ekşi, K. Y., Andaç, I. C., Çikintoğlu, S., et al. 2016, *ApJ*, 823, 34
- Espinoza, C. M., Lyne, A. G., & Stappers, B. W. 2017, *MNRAS*, 466, 147
- Foreman-Mackey, D., Hogg, D. W., Lang, D., & Goodman, J. 2013, *PASP*, 125, 306
- Gelman, A., & Rubin, D. B. 1992, *Statistical Science*, 7, 457
- Goldreich, P., & Julian, W. H. 1969, *Pulsar Electrodynamics*
- Gunn, J. E., & Ostriker, J. P. 1969, *Nature*, 221, 454
- Harding, A. K., Stern, J. V., Dyks, J., & Frackowiak, M. 2008, *ApJ*, 680, 1378
- Kou, F. F., & Tong, H. 2015, *MNRAS*, 450, 1990
- Kramer, M., Lyne, A. G., O'Brien, J. T., Jordan, C. A., & Lorimer, D. R. 2006, *Science*, 312, 549
- Landau, L. D., & Lifshitz, E. M. 1975, *The classical theory of fields*
- Lander, S. K., & Jones, D. I. 2018, *MNRAS*, 481, 4169
- Li, J., Spitkovsky, A., & Tchekhovskoy, A. 2012, *ApJ*, 746, 60
- Li, L., Tong, H., Yan, W. M., et al. 2014, *ApJ*, 788, 16
- Lyne, A., Graham-Smith, F., Weltevrede, P., et al. 2013, *Science*, 342, 598
- Lyne, A. G., Jordan, C. A., Graham-Smith, F., et al. 2015, *MNRAS*, 446, 857

- 354 Lyne, A. G., Pritchard, R. S., & Graham-Smith, F. 1993, MNRAS, 265, 1003
 355 Lyne, A. G., Pritchard, R. S., Graham-Smith, F., & Camilo, F. 1996, Nature,
 356 381, 497
 357 Magalhaes, N. S., Miranda, T. A., & Frajuca, C. 2012, ApJ, 755, 54
 358 Novoselov, E. M., Beskin, V. S., Galishnikova, A. K., Rashkovetskyi, M. M.,
 359 & Biryukov, A. V. 2020, MNRAS, 494, 3899
 360 Ostriker, J. P., & Gunn, J. E. 1969, Nature, 223, 813
 361 Padmanabhan, T. 2001, Theoretical Astrophysics - Volume 2, Stars and
 362 Stellar Systems
 363 Riley, T. E., Watts, A. L., Bogdanov, S., et al. 2019, ApJL, 887, L21
 364 Ruderman, M. A., & Sutherland, P. G. 1975, ApJ, 196, 51
 365 Spitkovsky, A. 2006, ApJL, 648, L51
 366 Tong, H., & Kou, F. F. 2017, ApJ, 837, 117
 367 Watters, K. P., Romani, R. W., Weltevrede, P., & Johnston, S. 2009, ApJ, 695,
 368 1289
 369 Xu, R. X., & Qiao, G. J. 2001, ApJL, 561, L85
 370 Yue, Y. L., Xu, R. X., & Zhu, W. W. 2007, Advances in Space Research, 40,
 371 1491